GROUND-TRUTH EVENTS FROM NORTHEASTERN AFRICA

Richard A. Brazier,[1] Yongcheol Park,[1] Andrew A. Nyblade,[1] and Michael E. Pasyanos[2]

Penn State University,[1] Lawrence Livermore National Laboratory[2]

Sponsored by National Nuclear Security Administration
Office of Nonproliferation Research and Engineering
Office of Defense Nuclear Nonproliferation

Contract No. DE-FC03-02SF22500[1] and W-7405-ENG-48[2]

ABSTRACT

Determining accurate seismic locations with representative uncertainty estimates is of fundamental importance to ground-based nuclear explosion monitoring. In this project, we are developing a catalog of reference events (ground-truth [GT]) in the northeast African area where reference event coverage is exceptionally poor due to the limited station coverage by historic networks. The results of this project will enable the seismic monitoring community to enhance their operational capability to monitor for nuclear tests in North Africa and the Middle East by increasing their ability to accurately locate and identify seismic events in these regions.

The collection of GT events for northeastern Africa is being achieved using state-of-the-art event location methods applied to broadband seismic data from regional networks in Ethiopia, Kenya and Tanzania, as well as to broadband data from primary and auxiliary International Monitoring System (IMS) stations in the region. The GT catalog is being assembled by determining origin time, focal mechanism and hypocenters for many events that lie within close proximity of recording stations or are well-recorded teleseismically.

Accurate event locations for fourteen M>3 events in northeastern Africa have been obtained so far using data from the Tanzania Broadband Seismic Experiment and the Ethiopia Broadband Seismic Experiment. Hypocenters have been constrained by using P and S arrival times, pP-P and sP-P times, and waveform modeling. Focal mechanisms for a subset of these events have also been obtained by modeling P and SH polarities and amplitude ratios in a grid search method.

INTRODUCTION

Determining accurate seismic locations with representative uncertainty estimates is of fundamental importance to ground-based nuclear explosion monitoring. In this project, we are developing a catalog of reference events (ground-truth[GT]) in northeast Africa where reference event coverage is exceptionally poor due to the limited station coverage by historic networks. We are developing a catalog of accurately located hypocenters within a range of GT levels, origin times, and focal mechanisms for several tens of earthquakes with magnitudes > 3. The catalog will enable the seismic monitoring community to enhance their operational capability to monitor for nuclear tests in North Africa and the Middle East by increasing their ability to accurately locate and identify seismic events in these regions.

Earthquakes in northeastern Africa provide a principal source of GT for North Africa and the Middle East. The earthquakes of interest are associated with the northern and central portions of the East African Rift System (Figure 1). Since there are very few earthquakes within North Africa proper or within large parts of the Middle East that can be used to develop a set of GT, naturally occurring events in northeastern Africa take on an added importance for improving nuclear explosion monitoring capabilities in the region.

The development of GT for North Africa and the Middle East has in the past been limited not only by the lack of appreciable seismicity but also by a dearth of seismic stations throughout most of Africa. This situation is now changing. We operated regional seismic networks in Ethiopia and Kenya comprised of 27 and 11 broadband stations, respectively, between 2000 and 2002, and several years ago (1994-1995) we operated a similar network of 20 broadband seismic stations in Tanzania. The broadband waveforms recorded by these networks, together with waveforms from primary and auxiliary IMS stations in the region, provide a rich dataset that can be used to accurately locate earthquakes and determine their origin times and source mechanisms.

The GT catalog is being assembled by (1) determining origin time, focal mechanism and hypocenters for many events that lie within close proximity of recording stations or are well recorded teleseismically; (2) using these events to construct regional travel time correction surfaces using a Bayesian kriging technique, and (3) using the travel time correction surfaces to obtain origin times and epicenters for numerous other events. Robust estimates of the uncertainties in the locations and origin times will also be determined.

Here we present improved locations for 11 events within Tanzania with M>4 and 3 events from Ethiopia with M > 3.5 constrained by P and S arrival times and pP, sP and Pmp depth phases recorded by the regional broadband networks in Tanzania and Ethiopia. We begin by providing background information about the geology of the region and on the broadband seismic experiments. This is followed by a discussion of our event locations and uncertainties, and we conclude with a brief description of future work.

Background Information

The locations of the broadband seismic experiments, together with the geology and topography of East Africa, are shown in Figure 1. The geology of the region is comprised of an Archean craton (the Tanzania Craton, Figure 1) surrounded Proterozoic mobile belts. The rift faults of the Cenozoic East African rift system have developed mainly within the Proterozoic mobile belts, forming a rift system with two branches (Western rift and Eastern rift).

The broadband seismic experiment in Tanzania was conducted in 1994 and 1995 and consisted of 20 seismic stations deployed for a year in two skewed arrays, one oriented more or less east-west, and the other northeast-southwest. The experiment was designed so that structure beneath the Archean Tanzania Craton and the terminus of the Eastern Rift in northern Tanzania could be imaged with seismic data from local, regional and teleseismic earthquakes. Information about the station configuration, recording parameters and other details of the field deployment has been reported by Nyblade et al. (1996).

In the other broadband seismic experiments, seismic stations consisting of broadband sensors, 24-bit data loggers, 4 Gbyte hard disks, and GPS clocks were deployed in regions of Ethiopia and Kenya that were safe for traveling (Figure 1). The stations were spaced 50 to 200 km apart and were located to optimize the recording of teleseismic body and surface waves that sample upper mantle structure beneath the Eastern Rift. For East Africa, the major source regions for teleseismic earthquakes are the Hindu Kush/Pamir region to the northeast and the Fiji/Tonga

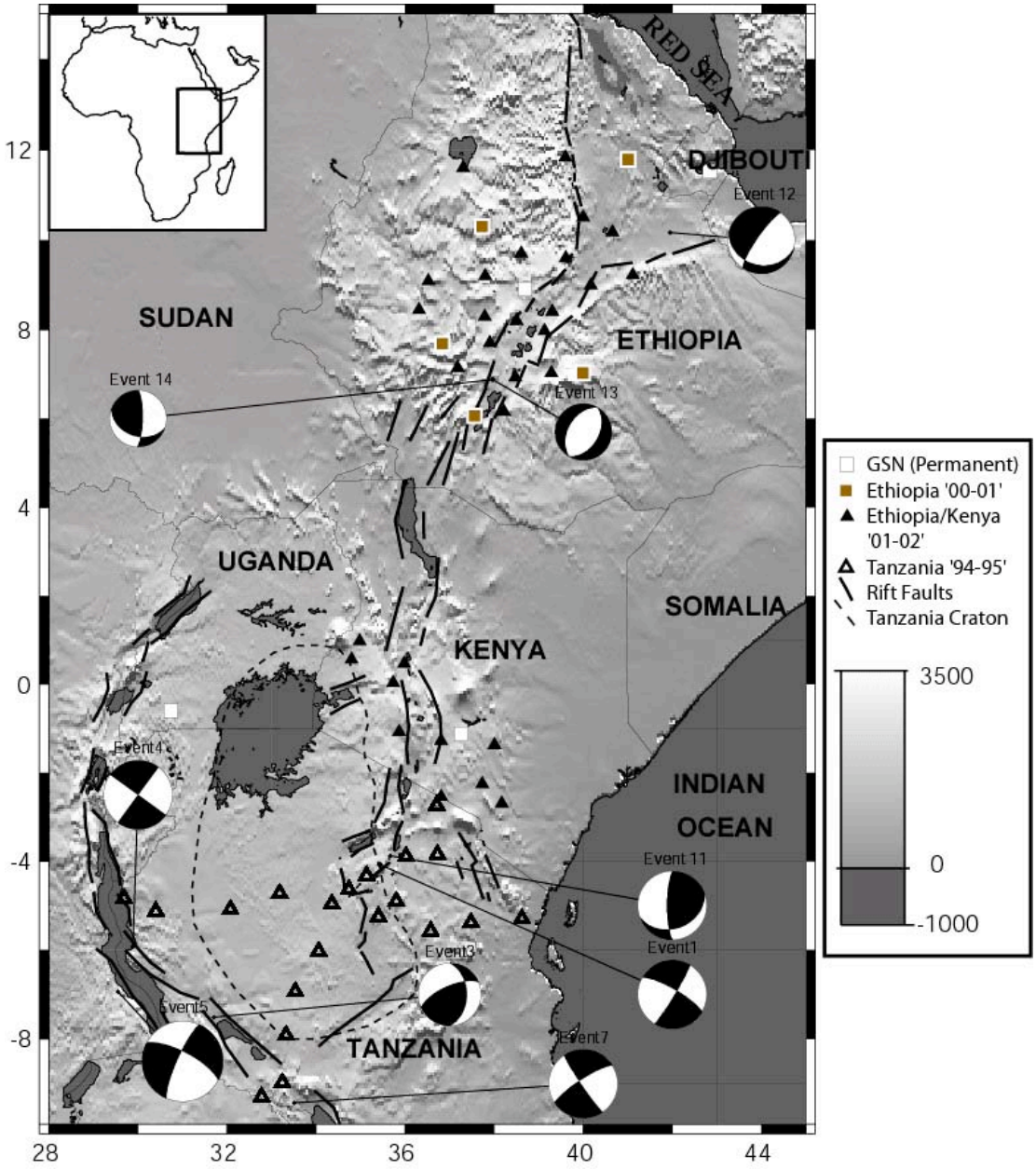

Figure 1. Topographic map of East Africa showing the Ethiopian and East African plateaus (regions with > 1000 m elevation), the outline of the Archean Tanzania craton, the major rift faults of the East African rift system, focal mechanisms for our events, and the location of broadband seismic stations.

subduction zones to the east. Additional criteria used for site selection included access to bedrock, security, and year-round road conditions.

Installation of the Ethiopian stations was completed in two phases. During March 2000, five stations were installed around the periphery of the network, and then one year later (March 2001) an additional 20 stations were installed to densify the network (Figure 1). All 25 stations were removed from the field in March 2002. Installation of the Kenyan stations took place during July and August 2001, and all 10 of the stations were removed in July 2002. Two data streams were recorded; a 1-sample/sec continuous stream and a 20 sample/sec continuous stream, yielding a data volume of 21 Mbytes per station per day.

Event Locations

Event locations have been obtained for several events in Tanzania with magnitudes $\geq$ 4 and in Ethiopia with magnitudes > 3.5 that were well recorded by the Tanzania and Ethiopia regional networks. The locations were obtained using P and S arrival times, a regional velocity model for both the crust and upper mantle constrained by a number of previous studies, and the event location code HYPOELLIPSE (Lahr, 1993). The P and S onset times were individually handpicked to within 0.1 seconds. The velocity models in Table 1 were used in the event location code for each respective region. The crust and uppermost mantle in East Africa have been studied in detail by many authors using refraction surveys, receiver functions, surface waves, regional waveforms and Pn tomography. From these studies, it is clear that Tanzania's crustal and uppermost mantle structure is fairly uniform in the Precambrian terrains away from the rift valleys proper (Last et al., 1997; Brazier et al., 2000; Nyblade, 2002; Langston et al., 2002; Fuchs et al. 1997 and references therein). Only minor differences in crustal thickness (2-5 km), mean crustal velocity (0.1-0.2 km/s), and uppermost mantle P velocities (0.1 – 0.2 km/s) are found between the various stations of the Tanzania network, and these differences introduce very small uncertainties in the event locations.

Table 1. Crust and uppermost mantle seismic structure for Tanzania and Ethiopia, East Africa.

	V1 (km/s)	V2 (km/s)	Poisson's Ratio	Moho Depth (km)	Mean crustal Vp (km/s)	Pn (km/s)
Tanzania	5.84	7.09	0.25	38	6.5	8.3
Ethiopia	6.2	6.99	0.25	44	6.4	8.0

V1= uppermost crustal velocity; V2=lowermost crustal velocity

Table 2 summarizes the event origin times and locations, and the uncertainties associated with the locations. All of the events are well recorded on at least 11 stations in Tanzania and 6 in Ethiopia. A number of the events are within a few tens of kilometers of a station and none are more than a few hundred kilometers from a station. The magnitude estimates for these events derive from using the maximum P wave amplitude within the first 5 seconds and the local magnitude scale for East Africa determined by Langston et al. (1998). Standard statistical measures at the 68% confidence interval in the error ellipse indicate that the hypocenters appear to be constrained to within a few kilometers. However, a detailed study of several of these events using regional waveform modeling (Langston et al., 2002) indicates that while the P and S arrival times do a fairly good job at constraining epicentral location, they do not provide tight constraints on source depth. Source depth for the events studied by Langston et al. (2002) are shown in Table 2. The source depth obtained from the P and S arrival times for these events differed from the source depths in Table 2 by 10 or more kilometers.

Focal mechanisms have been determined using polarities and amplitude ratios of local and regional P and S phases using the grid-search technique by Snoke (1984) and are plotted in Figure 1 and in Table 3. The focal mechanisms are then used with a wavenumber integration algorithm (Kennett, 1983) to compute full synthetic seismograms for several stations at several depths. The synthetics are compared against the data and regional depth phases such as pPn, sPn and PmP are used to constrain the source depths. In Figure 2, we show the P wave train from the vertical component for the Lake Tanganyika event of November 12th 1994 (event 5), from two stations, RUNG at 402 km and KIBA at 766 km from the source. These traces are reduced to the Pn velocity. The depth phase sPn aligns best with the data and synthetics for a 18 km source depth. Fixing the depth of this event at 18 km, and then relocating using the arrival times, gives a more accurate location overall.

For comparison, we also show in Table 2 the locations and origin times for several of the events taken from the ISC catalog and earlier locations obtained without using depth phases to constrain focal depths. Locations for two events were also determined using data from stations outside of our networks in East Africa. The comparison shows discrepancies in origin times of several seconds in most cases, and differences in event location of many tens of kilometers for some events. In addition, no catalog listings were found for several of the events.

Future Work

In future work, we will focus on obtaining more accurate hypocenters for the regionally recorded events in Tanzania and Ethiopia. Preliminary locations using P travel times for several events in Ethiopia are given in Table 4.

In all of these steps it is crucial to have good velocity models for the crust and upper mantle. We will use analyses of receiver functions, surface waves and seismic refraction profiles to provide independent estimates of crustal and

Table 2. Locations for earthquakes in East Africa with M > 4 from July 1994 – June 1995 recorded by the Tanzania Broadband Seismic Experiments and from April 2000 - March 2002 recorded by the Ethiopia Broadband Seismic Experiment.

Event:source	yr:mo:day:hr:min:sec	Lat.	Lon.	Dep	M	N	Gap	RMS	Smaj	Az	Smin	Sez
1:Traveltimes	94:07:20:11:32:04.30	-4.080	35.440	42	4.5	19	141	0.44	0.25	-106	0.45	1.7
1:ISC	94:07:20:11:31:58.49	-4.171	35.185	0	3.8			1.26	10.4	90	6.6	
1:Fixed Depth	94:07:20:11:32:02.79	-4.251	35.585	15+	4.5	19	132	2.34	0.22	-108	0.35	0.49
2: Fixed Depth	94:08:18:00:45:48.80	-7.440	31.770	25*	5.9+	17	167	1.77	0.35	-34	0.48	2*
2: ISC	94:08:18:00:45:52.70	-7.650	31.830	25	5.9			0.69	2.20	90	2.20	
3: Traveltimes	94:09:05:04:08:56.04	-7.508	31.700	?	4.1	15	174	0.43	0.41	-59	0.70	?
3: ISC	94:09:05:04:08:50.41	-7.738	30.882	4	4.6			1.38	10.9	90	6.3	
3. Fixed Depth	94:09:05:04:08:54.83	-7.502	31.700	18+	4.1	18	174	0.54	0.38	-50	0.55	2*
4: Traveltimes	94:09:30:01:36:53.14	-5.920	29.890	26	4.5	16	229	1.13	0.55	-40	1.18	1.4
4: ISC	94:09:30:01:36:47.62	-8.426	37.261	0	4.4			1.78	15.6	90	8.6	
4: Fixed Depth	94:09:30:01:36:55.54	-5.876	30.202	11	4.5	16	210	1.50	0.82	-4	1.03	2.1
5: Traveltimes	94:11:12:12:18:00.00	-6.950	29.920	30*	5.3	16	179	0.55	0.42	-24	0.89	2*
5: ISC	94:11:12:12:18:01.33	-6.777	29.821	22	4.6			1.05	6.3	90	4.5	
5. Fixed Depth	94:11:12:12:18:00.88	-6.708	30.111	18+	5.3	16	179	0.95	0.39	-26	0.74	2+
5. Fixed Depth plus additional data	94:11:12:12:17:57.73	-6.939	29.552	18+	5.3	23	94	2.13	0.31	-40	0.36	2+
6: Traveltimes	94:11:12:20:16:59.37	-6.617	30.016	?	4.7	17	223	0.88	0.45	-33	0.96	?
6: ISC	94:11:12:20:16:49.66	-6.834	29.946	0	4.6			1.15	8.4	90	5.5	
6. Fixed Depth	94:11:12:20:16:58.59	-6.652	30.135	8+	4.7	20	211	1.29	0.39	-26	0.73	2+
7: Traveltimes	94:11:16:01:08:11.20	-9.070	33.330	8*	4.5	17	193	0.80	0.48	-129	0.66	2*
7: ISC	94:11:16:01:08:09.07	-9.179	33.273	10	5.0			1.64	7.8	90	6.8	
7: Fixed Depth	94:11:16:01:08:10:21	-9.145	33.454	7+	4.5	17	204	0.86	0.51	-112	0.73	2+
7: Fixed Depth plus additional data	94:11:16:01:08:05.78	-9.424	33.513	7+	4.5	20	150	3.6	0.29	-52	0.54	0.97
8: Traveltimes	94:11:27:04:20:51.65	-3.568	35.827	30	4.0	15	213	0.51	0.36	-93	0.95	0.7
8: ISC	94:11:27:04:20:44.27	-3.954	35.722	10	4.0			0.12	22.4	90	10.1	
9: Traveltimes	94:12:25:04:25:27.44	-5.113	29.752	21	4.2	11	301	0.59	0.81	19	6.42	1.9
9: ISC	No listing											
10: Traveltimes	95:01:29:00:23:35.02	-5.419	35.909	13	4.1	11	128	0.37	0.34	-107	0.51	1.0
10: ISC	No listing											
11: Traveltimes	95:02:12:16:37:30.00	-3.960	35.830	32*	4.5	20	?					2*
11: ISC	No listing											
11: Fixed Depth	95:02:12:16:37:33.85	-3.879	35.670	34+	4.5	13	215	0.56	0.36		0.96	2+
12: ISC	00:05:16:20:47:51.93	10.10	41.23	10	4.4							
12: Fixed Depth	00:05:16:20:47:51.27	10.17	41.95	7+	4.4	6	166	1.72	0.49	-120	1.25	3.45
13: Traveltimes	01:03:11:00:42:43.58	6.91	38.01	0.02	3.7	13	78	1.57	0.26	-64	0.3	0.87
13: Fixed Depth	01:03:11:00:42:41.88	6.88	37.96	4+	3.7	7	92	0.41	0.35	-69	0.37	2.91
14: Traveltimes	01:03:12:16:40:08.92	6.78	37.98	0	3.7	9	128	2.79	0.31	-82	0.42	0.94
14: Fixed Depth	01:03:12:16:40:07.23	6.88	37.97	5+	3.7	7	92	0.40	0.35	-74	0.37	1.09

D = depth in km. * = depth was determined from regional depth phases (Langston et al., 2002). Otherwise depths were determined from only P and S arrival times.

M = magnitude. Magnitudes in this study are based on the ML scale from Langston et al. (1998). ISC magnitudes are a mixture of different types.

N = number of stations used in the event location.

Gap = azimuth range in stations.

RMS = Rms error in arrival times.

Smaj, Smin, Sez, Az = dimensions (in kms) and orientation of the error ellipse. For this study, the numbers in the table are for a 68% confidence level. * on Sez numbers indicates that the depth uncertainty was obtained from modeling regional depth phases (Langston et al., 2002).

mantle velocities. In addition, we will make surface wave dispersion measurements of data from the three regional networks in the area. We are measuring both Love and Rayleigh surface wave group velocities using a multiple narrow-band filter technique. Combined with thousands of other measurements made in the broader regional area (Pasyanos et al., 2001), we will conduct a high-resolution group velocity tomography of northeastern Africa. Using near-regional data will enable us to make more accurate short-period (5-15 seconds) measurements that will allow us to constrain velocities in the uppermost crust. We will use the surface wave work, along with receiver functions and other data, to improve the velocity model of the crust and upper mantle and in turn improve the event locations.

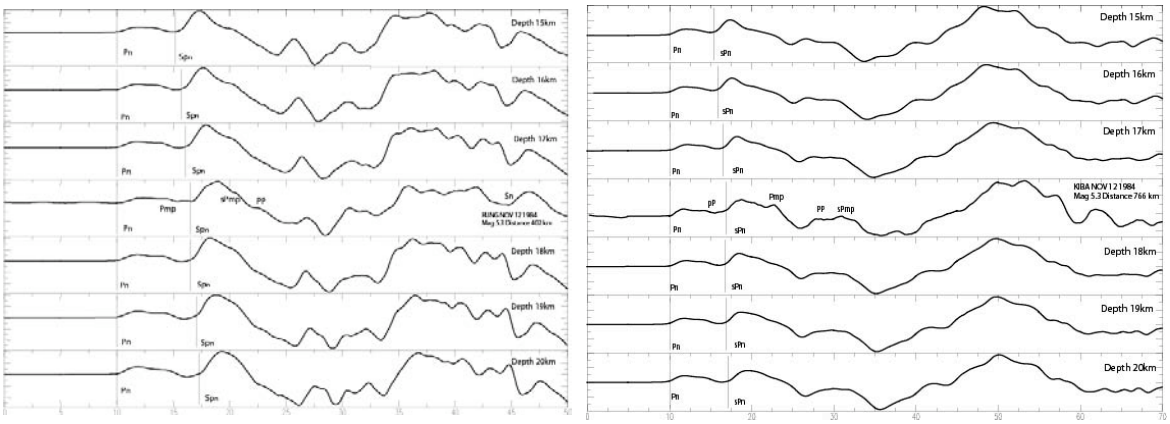

Figure 2. Data from November 12th 1994 Tanganika event recorded at (a) RUNG and synthetics for source depths 15 –20 km, and (b) Data from November 12th 1994 Tanganika event recorded at KIBA and synthetics for depths at 15 –20 km

Table 3. Focal mechanisms for events in Table 2.

	Strike (deg)	Dip (deg)	Rake (deg)
Event 1	300	77	-5
Event 3	0	45	32
Event 4	36	335	-10
Event 5	204	79	-19
Event 7	146	85	-11
Event 11	180	77	59
Event 12	102	26	-25
Event 13	210	45	-90
Event 14	109	38	22

To expand the catalog of events in northeastern Africa, we will take the events located using the approach described above and use them as calibration events to construct travel-time correction surfaces using the kriging method of Schultz et al., (1998, 1999) and Myers and Schultz (2000). The travel-time correction surfaces will then be used with local and regional P arrivals to determine epicenters and origin times for numerous other events in the Ethiopia, Kenya and Tanzania datasets. Based on the expected proximity of many of these events to recording stations, we anticipate that there will be many events whose epicenters will be determined to within 10 km.

The travel-time correction surfaces will be constructed following the approach outlined by Myers and Schultz (2000). For the regional networks, we will calculate travel-time residuals for the calibration events relative to a regional velocity model. The travel-time residuals will be assigned to the respective calibration epicenter and form a set of spatially varying travel-time correction points. This set of points will then be declustered to reduce the dimensions of the observations, and this refined set of calibration points will be used with Bayesian kriging to form continuous travel-time surfaces that will provide source-specific corrections for each station in the regional networks. In locating epicenters, a standard location algorithm will be used with the kriging corrections applied. A

Table 4. Locations for earthquakes in Ethiopia with M > 2 from April 2000 to March 2002.

Event:source	yr:mo:day:hr:min:sec	Lat.	Lon.	Dep	M	N	Gap	RMS	Smaj	Az	Smin	Sez
1:Traveltimes	01:04:03:17:40:27.84	15.008	40.990	?	3.9	18	286	5.74	21.08	-70	4.29	?
2: Traveltimes	01:04:04:01:00:21.84	13.534	39.913	?	3.2	22	276	1.76	3.72	-78	0.92	4.22
3: Traveltimes	01:04:05:12:50:14.29	11.848	40.856	15	3.3	9	190	6.08	6.65	-89	1.28	1.12
4: Traveltimes	01:04:06:16:36:30.99	11.403	39.659	?	3.6	23	82	2.06	2.10	-51	0.72	4.97
5: Traveltimes	01:04:09:10:49:52.44	7.565	38.843	15	2.8	4	139	0.73	?	-25	0.83	?
6: Traveltimes	01:04:11:20:33:49.85	12.15	39.683	15	3.0	10	258	9.06	12.6	-54	3.38	2.53
7: Traveltimes	01:04:12:11:50:57.28	6.65	38.067	15	2.9	6	135	1.97	9.52	-43	0.53	15.1
8: Traveltimes	01:04:14:23:40:27.86	8.979	39.95	15	2.9	19	101	7.94	1.3	-49	0.77	3.1
9: Traveltimes	01:04:20:06:16:40.62	9.589	39.641	15	2.4	4	193	0.44	28.79	-60	1.68	18.0
10: Traveltimes	01:04:20:19:02:0073	5.593	37.187	15	2.8	7	288	0.91	13.8	-52	1.34	8.51
11: Traveltimes	01:04:21:20:41:37.81	11.213	42.617	15	2.7	8	177	4.21	19.06	-16	3.62	?
12: Traveltimes	01:04:24:01:58:35.01	14.218	40.912	15	3.3	16	272	5.92	12.03	-85	3.4	?
13: Traveltimes	01:04:24:21:56:28.42	10.122	42.867	15	3.2	14	224	2.33	12.74	0	2.57	15.4
14: Traveltimes	01:04:25:19:26:19.86	11.575	40.964	15	3.2	14	89	2.52	2.84	-100	0.9	3.88
15: Traveltimes	01:04:25:21:12:25.76	7.553	44.198	15	4.1	17	276	8.62	2.16	24	0.55	?
16: Traveltimes	01:04:27:22:43:44.46	6.203	37.684	15	2.1	8	144	2.27	7.1	-47	2.18	3.85
17: Traveltimes	01:04:27:17:39:12.21	6.067	37.556	15	2.5	3	252	?	?	4	2.19	?
18: Traveltimes	01:05:03:13:39:55.53	13.847	41.076	10	3.8	17	265	2.98	2.00	-78	0.60	?
19: Traveltimes	01:05:04:17:26:22.00	12.786	41.239	10	3.7	10	236	2.47	1.37	-82	0.56	1.63
20: Traveltimes	01:05:07:00:16:12.46	7.010	45.689	10		6	360	0	10.03	-133	1.12	99
21: Traveltimes	01:05:07:10:32:49.81	0.795	41.022	10		3	360	0	9.44	30	0.85	99
22: Traveltimes	01:05:12:01:44:16.07	9.508	39.691	0.02	3.6	11	123	2.32	0.46	-34	0.35	0.86
23: Traveltimes	01:05:17:07:24:01.24	11.410	42.942	0	3.6	11	252	6.72	4.48	-24	0.77	3.47
24: Traveltimes	01:05:17:09:24:55.33	11.770	42.893	10	3.6	8	279	5.46	5.21	-27	0.85	1.18
25: Traveltimes	01:05:18:18:07:55.44	5.539	36.081	10	4.0	18	143	6.23	0.66	22	0.34	?
26: Traveltimes	01:05:19:17:54:28.67	8.629	39.504	325	4.4	21	119	5.13	0.76	31	0.43	2.05
27: Traveltimes	01:05:19:18:49:18.28	11.773	43.200	10	3.7	15	308	7.29	5.27	-25	0.82	1.9
28: Traveltimes	01:05:22:09:20:52.26	7.586	45.386	10	4.1	13	256	13.5	1.82	2	0.56	?
29: Traveltimes	01:05:23:01:16:12.76	2.639	49.772	10	4.1	24	60	2.81	0.29	-132	0.21	0.63
30: Traveltimes	01:05:25:05:14:29.10	21.059	39.799	10	4.4	14	291	5.60	3.81	18	0.86	?

D = depth in km.

M = magnitude. Magnitudes in this study are based on the ML scale from Langston et al. (1998).

N = number of stations used in the event location.

Gap = azimuth range in stations.

RMS = Rms error in arrival times.

Smaj, Smin, Sez, Az = dimensions (in kms) and orientation of the error ellipse. For this study, the numbers in the table are for a 68% confidence level.

conservative uncertainty estimate for the kriging correction will be used to characterize the travel-time-prediction error, according to the procedure followed by Myers and Schultz (2000). This conservative estimate will be developed using rigorous statistical modeling with available seismic data. Cross-validations will be provided to ensure that the estimates are accurate. In general, these statistics will be used as input to generate chi-squared values for robustly determining the final reference event error ellipses.

REFERENCES

Brazier, R., A.A. Nyblade, C. A. Langston, and T.J. Owens, Pn velocities beneath the Tanzania Craton and adjacent rifted mobile belts, East Africa, *Geophys. Res. Lett.*, 27, 2365-2368, 2000.

Fuchs, K., Altherr, B., Muller, B., and Prodehl, C., Structure and dynamic processes in the lithosphere of the Afro-Arabian rift system: *Tectonophysics, 278*, 1-352, 1997.

Kennett, B.N.L., Seismic wave propagation in stratified media, *Cambridge University Press*, 1983.

Lahr, J.C., Hypoellipse, a computer program for determining local earthquake hypocentral parameters, magnitude and first motion pattern, U.S. Geological Survey Open File Report 89-116, 1993.

Langston, C.A., R. Brazier, A.A. Nyblade and T. J. Owens, Local magnitude scale and seismicity rate for Tanzania, East Africa, *Bull. Seis. Soc. Am., 88*, 712-721, 1998.

Langston, C.A., A.A. Nyblade, and T.J. Owens, Regional wave propagation in Tanzania, East Africa, *J. Geophys. Res.*, 107, 10.1029, 2002.

Last, R., A.A. Nyblade, C.A. Langston, and T.J. Owens, Crustal structure of the East African plateau from receiver functions and Rayleigh wave phase velocities, *J. Geophys. Res., 102*, 24469-24483, 1997.

Myers, S., and C. Schultz, Improving sparse network seismic location with Bayesian kriging and teleseismically constrained calibration events, *Bull. Seis. Soc. Am., 90*, 199-211, 2000.

Nyblade, A.A., C. Birt, C. A. Langston, T.J. Owens, and R. J. Last, Seismic experiment reveals rifting of craton in Tanzania, *Eos Trans. AGU, 77*, 517-521, 1996.

Nyblade, A.A., Crust and upper mantle structure in East Africa and the origin of Cenozoic extension, magmatism and plateau uplift, in *Magmatic Rifted Margins*, edited by M. Menzies, C. Ebinger and S. Klemperer, Geological Society of America special paper 362-0, in press, 2002.

Pasyanos, M.E., W.R. Walter, and S.E. Hazler, A surface wave dispersion study of the Middle East and North for monitoring the Comprehensive Nuclear-Test-Ban Treaty, *Pure and Applied Geophysics*, 2001.

Schultz, C., S. Myers, J. Hipp, and C. Young, Nonstationary Bayesian kriging: a predictive technique to generate spatial corrections for seismic detection, location and identification, *Phys. Earth. Planet. Int., 113*, 321-338, 1999.

Schultz, C., S. Myers, J. Hipp, and C. Young, Nonstationary Bayesian kriging: a predictive technique to generate spatial corrections for seismic detection, location and identification, *Bull. Seis. Soc. Am., 88*, 1275-1288, 1998.

Snoke, J.A., Munsey, J W; Teague, Alan G; Bollinger, G A. A program for focal mechanism determination by combined use of polarity and SV-P amplitude ratio data, *Seismological Society of America, Eastern Section, 56th annual meeting, Earthquake Notes, vol.55, no.3, pp.15, Sep* 1984.